HHS Public Access

Author manuscript

ACS Appl Mater Interfaces. Author manuscript; available in PMC 2022 January 27.

Published in final edited form as:

ACS Appl Mater Interfaces. 2019 May 15; 11(19): 17184–17192. doi:10.1021/acsami.9b01218.

Liposome-Encapsulated Curcumin-Loaded 3D Printed Scaffold for Bone Tissue Engineering

Naboneeta Sarkar, **Susmita Bose***

W. M. Keck Biomedical Materials Research Laboratory, School of Mechanical and Materials Engineering, Washington State University, Pullman, Washington 99164, United States

Abstract

Curcumin, the active constituent for turmeric, is known for its antioxidant, anti-inflammatory, anticancer, and osteogenic activities. However, it shows extremely poor bioavailability, rapid metabolism, and rapid systemic elimination. In this study, we have increased the bioavailability of curcumin by encapsulating it in a liposome, followed by the incorporation onto 3D printed (3DP) calcium phosphate (CaP) scaffolds with designed porosity. 3DP scaffolds with a designed shape and interconnected porosity allow for the fabrication of patient-specific implants, providing new tissue ingrowth by mechanical interlocking between the surrounding host tissue and the scaffold. Upon successful encapsulation of curcumin into the liposomes, we have investigated the effect of liposomal curcumin released from the 3DP scaffolds on both human fetal osteoblast cells (hFOB) and human osteosarcoma (MG-63) cells. Interestingly, liposomal curcumin released from the 3DP scaffold showed significant cytotoxicity toward in vitro osteosarcoma (bone cancer) cells, whereas it promoted osteoblast (healthy bone cell) cell viability and proliferation. These results reveal a novel approach toward the fabrication of tissue engineering scaffolds, which couples the advanced additive manufacturing technology with the wisdom of alternative medicine. These bifunctional scaffolds eradicate the osteosarcoma cells and also promote osteoblast proliferation, offering new opportunities to treat bone defects after tumor resection.

Graphical Abstract

***Corresponding Author** sbose@wsu.edu. Phone: (509) 335-7461.

The authors declare no competing financial interest.

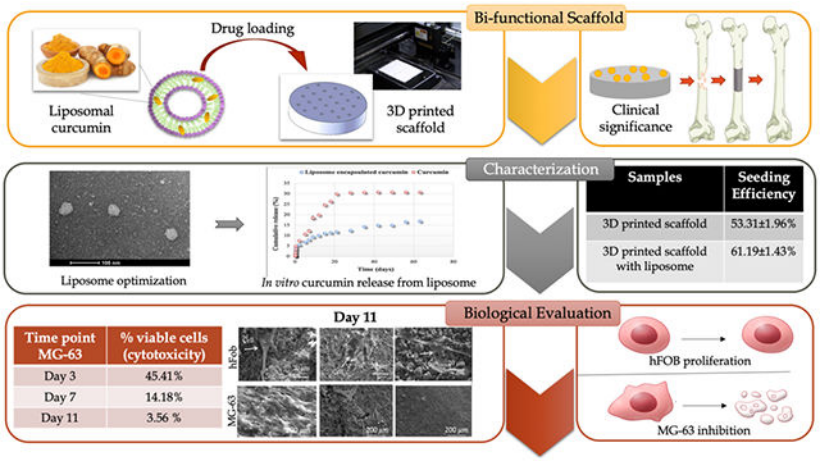

Keywords

curcumin; liposome; 3D printing; osteosarcoma; osteoblast

1. INTRODUCTION

Curcumin is a hydrophobic, polyphenolic compound derived from the rhizome of the turmeric herb (*Curcuma longa*).[1] It is mostly consumed in southeast Asian countries as a culinary spice and has been used in Indian Ayurvedic medicine for centuries. Modern scientific research has shown curcumin's efficacy toward cancer, arthritis, diabetes, multiple sclerosis, the common cold, inflammation, and indigestion.[2-5] It has also shown significant in vitro and in vivo chemopreventive potential for various forms of cancers including leukemia, melanoma, lymphoma, breast cancer, ovarian cancer, lung cancer, and bone cancer.[6-10]

Unlike other forms of cancer, bone cancers and its subtypes are generally detected during the first decades of life and are considered the most prevalent primary bone malignancy.[11] It is the second most prevalent cause of cancer death among young adults following leukemia. Adolescent cancers like this are often treated with high doses of anticancer drugs compared to those in adults, which increase the risk of short- and long-term side effects.[12] The current standard for the treatment of bone cancer involves preoperative and/or postoperative chemotherapy along with surgery.[13] However, postsurgical defect repair while suppressing tumor regrowth is considered a major concern, motivating investigations for alternative treatment methods.

Bone scaffolds have shown their potential to repair postsurgical critical-sized defects by providing better physical support and a favorable biocompatible environment for in vivo tissue formation.[14,15] Three-dimensional printed (3DP) tissue engineering scaffolds are considered as an excellent choice for bone graft substitutes because of their control over pore geometry, connectivity, and chemistry. The interconnected pores facilitate nutrient transportation, continuous ingrowth of new bone, vascularization, and waste product removal.[16,17] Furthermore, 3D printing is the only manufacturing technique which can

synthesize patient-specific anatomical replicas from a detailed patient scan. In this study, the 3DP scaffolds were synthesized from tricalcium phosphate (TCP) ceramics. TCP is a group of calcium phosphate ceramics, which is well-known for its good bioactivity, homogeneous osteoconductivity, and compositional similarity to the bone.[18-21]

The therapeutic efficacy of these scaffolds can be enhanced when anticancer drugs or growth factors are incorporated within it. Current anticancer therapies involve monotargeted approaches, which are not considered as effective as multitargeted preventions. Additionally, synthetic anticancer drugs are often toxic toward normal cells along with cancer cells, which cause serious side effects. Natural biomolecules derived from plant-based products not only exhibit multitargeted modulation but also are inexpensive and safer alternatives to synthetic drugs.[10] Numerous in vitro and in vivo reports suggest the antitumor effects of curcumin toward osteosarcoma cells and explain its underlying mechanism. Curcumin induces apoptosis in bone cancer cells via multiple pathways, including the inhibition of nuclear factor-$\kappa\beta$ (NF-$\kappa\beta$) and the expression of interleukin-6 (IL-6) and IL-11, the inhibition of tumor-induced angiogenesis by downregulating vascular endothelial growth factor and matrix metalloproteinases-9 (MMP-9), and the inhibition of extracellular signal-regulated kinase expression.[22,23] An in vivo study in rats shows that treatment with curcumin and cisplatin, an antitumor drug, exhibits regulation over the tumor marker of the cancerous cells compared to normal cells.[24] Another study in mice showed that curcumin therapy along with radiotherapy resulted in higher apoptosis of cancer cells and lowered radioresistance.[25]

Regardless of its widespread therapeutic efficacy, curcumin exhibits poor bioavailability because of its limited water solubility.[26] Also, it shows rapid intestinal and hepatic metabolism which results in an elimination of 60–70% through the bowel.[27] Various drug carriers have been designed to improve the bioavailability of curcumin, among which liposomes are the most common, well-investigated, and promising mode of drug delivery system.[28,29] These are biocompatible, biodegradable, nontoxic spherical vesicles with an effective drug delivering ability. Not only do they improve the cellular and tissue uptake but also enhance the distribution of the therapeutic compounds to the target sites.[30] These phospholipid nanovesicles can encapsulate both hydrophobic and hydrophilic drugs. Hydrophobic or lipophilic drugs are entrapped within the bilayer membrane, whereas hydrophilic drugs are inserted in the aqueous center.[31]

This study presents the successful encapsulation of the hydrophobic biomolecule curcumin within a liposome and the incorporation of the liposome within a 3DP TCP scaffold. The scaffold provides mechanical support for cell attachment, and prolonged drug release from the liposome helps achieve improved bioavailability, better therapeutic index, and lowered toxicity. This study introduces us to an era of integration, where modern 3DP technology is coupled with the safe and effective use of alternative medicine, which may provide a better tool for bone tissue engineering. Results showed that curcumin-encapsulated liposomes in a 3DP bone tissue engineering scaffold inhibit in vitro osteosarcoma cells by 96% compared to untreated samples. It also exhibited no cytotoxicity toward healthy osteoblast cells, promoting adhesion, proliferation, and formation of filopodial prostheses on the scaffold surface.

2. EXPERIMENTAL SECTION

2.1. Preparation and Characterization of Curcumin-Encapsulated Liposomes.

Curcumin-encapsulated liposomes were prepared by thin-film hydration method. Briefly, curcumin [≥94% (curcuminoid content), ≥80% (curcumin), Sigma-Aldrich, USA] was dissolved in dimethyl sulfoxide (DMSO). The lipids, 1,2-dimyristoyl-*sn*-glycero-3-phosphocholine (DMPC, Avanti Polar Lipids, Alabama, USA) and 1,2-dimyristoyl-*sn*-glycero-3-phospho-(1′-*rac*-glycerol) (sodium salt) (DMPG, Avanti Polar Lipids, Alabama, USA) were dissolved in *tert*-butanol in a ratio of 7:3. The total lipid-to-curcumin ratio was optimized at 15:1. The two solutions were mixed and placed in lyophilization vials. The vials were frozen by immersing in a liquid nitrogen bath and then lyophilized for 48 h at −52 °C to remove all DMSO and *tert*-butanol. A thin lipid film was formed, which was dissolved in deionized (DI) water. The solution was filtered through a 0.22 μM filter for sterilization.

The unentrapped drug was separated by centrifuging the liposome suspension at 32 645*g* for 50 min. The percentage encapsulation efficiency was investigated by ultrasonicating the supernatant solution for 10 min in the presence of ethanol. The concentration of curcumin was determined spectrophotometrically at a wavelength of 427 nm using a microplate reader.

$$\text{Encapsulation efficiency of curcumin (\%)} = \frac{\text{curcumin entrapped in liposome}}{\text{total curcumin added for liposome preparation}} \times 100$$

The liposome microstructure was characterized by transmission electron microscopy (TEM) using the negative stain method. The samples were diluted before preparing for TEM. A drop of the diluted solution is taken and placed on a copper grid coated with carbon film. It was air-dried and then stained with uranyl acetate. After drying at room temperature overnight, TEM was done.

2.2. 3DP Scaffold Preparation.

The solid-state synthesis was carried out to prepare pure ß-TCP powder. Briefly, 1 M calcium carbonate ($CaCO_3$) and 2 M calcium phosphate dibasic ($CaHPO_4$) were mixed and ball-milled for 2 h to obtain a homogeneous mixture. Calcination was performed at 1050 °C for 24 h. The calcined powder was sieved and then ball-milled with 2:3 w/v ethanol (200 proof, Decon Labs, PA) using a 5:1 ball–to-powder ratio. After 6 h, ethanol was evaporated at 60 °C by keeping the slurry in a conventional furnace overnight. The synthesized powder was sieved and then used to fabricate 3DP scaffolds using a binder jet printer (ProMetal, ExOne LLC, Irwin, PA, USA). Cylindrical scaffolds with 3.2 mm diameter and 5 mm height along with interconnected 3D pores were designed by computer-assisted design (CAD). The designed pore size was 400 μm, where the square-shaped pores penetrate orthogonally through the cylinder in *X*, *Y*, and *Z* directions. For in vitro cell culture, scaffolds were specifically designed with 12.5 mm diameter and 2 mm height with a designed pore size of 200 μm. These scaffolds were intentionally designed to have unconnected and discrete designed pores so that the cells do not wash away through the pores or adhere to the pore walls making them difficult to image. Some important process parameters, such as layer

thickness, drying power, and saturation, were optimized depending on part geometry and powder morphology. The aqueous binder used for printing was proprietary and provided by ProMetal, ExOne LLC, Irwin, PA, USA. Binder removal was carried out at 175 °C for 90 min. A depowderization process by air-blowing was performed to remove loosely adhered powder, which was blocking the pores. The sintering of the scaffolds was carried out at 1250 °C in a conventional muffle furnace for 2 h. Figure 1 demonstrates the fabrication of TCP scaffold and curcumin-encapsulated liposome via 3D printing and thin-film hydration method, respectively.

2.3. In Vitro Liposome-Encapsulated Curcumin Release.

For in vitro curcumin release study, dialysis tubings (MW cutoff 12 000–14 000 Da) were purchased from Carolina biological, NC, USA. They were soaked in DI water overnight to remove the preservatives. Subsequently, two dialysis sacs were prepared: one with free curcumin as control and the other containing liposomal curcumin. Phosphate-buffered saline (PBS) (pH 7.4) was prepared with 25% v/v methanol. The sacs were tightly closed with a thread and immersed in the buffer solution using a glass rod. The flask was kept at 37 °C and stirred at 150 rpm with a magnetic stirrer. The samples were collected after selected time points, and absorbance was measured using a BioTek Synergy 2 SLFPTAD microplate reader (BioTek, Winooski, VT, USA).

2.4. In Vitro Osteoblast and Osteosarcoma Cell Culture Study.

Prior to the in vitro cell culture study, all scaffolds were sterilized using an autoclave (Tuttnauer, USA) at 121 °C for 60 min. Human osteosarcoma cell line (MG-63) and Eagle's minimum essential medium (EMEM) were purchased from ATCC, USA. The cell culture medium or EMEM was replaced every 2–3 days during the entire study. Subsequently, the sterilized scaffolds were loaded with liposomal curcumin and placed in 24-well plates. Confluent cells were seeded on the scaffold surface at a density of 2.5×10^4 cells/sample. The scaffolds were moved to a new well after an adhesion period of 12 h. The culture was kept in an incubator at 37 °C under an atmosphere of 5% CO_2 as recommended by ATCC for this particular cell line.

Human fetal osteoblast cell (hFOB) line and osteoblast growth medium were purchased from PromoCell GmbH, Germany. 3DP scaffolds incorporated with liposomal curcumin were placed in 24-well plates and the cells were seeded onto the scaffolds at a density of 2×10^4 cells/sample. Seeding efficiency was carried out after 12 h, and the scaffolds were moved to a new well after an adhesion period of 12 h. MTT (3-(4,5-dimethylthiazol-2-yl)-2,5-diphenyl tetrazolium bromide) assay was utilized to determine the cell seeding efficiency after 12 h of incubation, using the following equation.

For a scaffold,

$$\text{Cell seeding efficiency}\,(\%) = \frac{\text{optical density of cell-seeded on the scaffold}}{\text{optical density of total cells used for seeding}} \times 100$$

The culture was kept at 37 °C under an atmosphere of 5% CO_2 in an incubator as suggested by PromoCell for this specific cell line. The medium was refreshed every 2–3 days until the 11-day time point was reached.

2.5. MTT Cell Viability Assay and Cellular Morphology.

To evaluate the seeding efficiency and cell viability, MTT assay (Sigma, St. Louis, MO) was carried out at 3, 7, and 11 days. The time points were chosen based on the principal development stages of hFOB: attachment (1–3 days), proliferation period (6–7 days), and mineralization or differentiation (11 days). MTT assay is a widely accepted colorimetric assay, which reflects the number of viable cells present in the system. The yellow tetrazolium dye or MTT is reduced by metabolically active cells by the action of mitochondrial oxidoreductase enzymes. The resultant product is a purple-colored formazan crystal, which is solubilized and quantified spectrophotometrically. The MTT reagent was dissolved in sterile filtered PBS at a concentration of 5 mg/mL to make the MTT solution. Three scaffolds of each composition were used at each time point, and they were discarded after performing the assay. At each time point, the scaffolds were taken out and 100 μL of the MTT solution was added on top of each scaffold in the 24-well plates. After 2 h of incubation, 600 μL of MTT solubilizer (10% Triton X-100, 0.1 N HCl, and isopropanol) was added for dissolving the formazan crystals. A 100 μL of the solution was added to the 96-well plates and optical density was measured using a microplate reader at 570 nm. To determine the cytotoxicity for the osteosarcoma cell line, the percentage cell viability was calculated using the following equation

$$\text{Cell viability (\%)} = \frac{\text{mean value of the measured optical density of test sample}}{\text{mean value of the measured optical density of the control}} \times 100$$

For cellular morphology by field emission scanning electron microscopy (FESEM), the samples were taken from the culture after 3, 7, and 11 days of study. To fix the samples overnight, 2% paraformaldehyde/2% glutaraldehyde in 0.1 M cacodylate buffer was used at 4 °C. Postfixation was carried out using 2% osmium tetroxide (OsO_4) for 2 h at room temperature. Then, the samples were rinsed with fresh buffer solution three times. A series of ethanol concentrations in distilled water (30, 50, 70, 95, and 100% ethanol) were prepared to carry out the dehydration procedure. Starting with the lowest concentration of ethanol solution, the process was continued until the samples are in 100% ethanol. In each step, the samples were left in the ethanol solution for 10–15 min. After repeating the 100% ethanol step, the samples were subjected to overnight hexamethyldisilane drying. Afterward, a gold coating with a thickness of 10–15 nm was applied using a gold sputter coater. The cellular morphology on the sample surface was characterized by FESEM (FEI 200F, FEI Inc., OR, USA).

2.6. Alkaline Phosphatase Osteoblast Cell Differentiation Assay.

Osteoblastic differentiation was evaluated by alkaline phosphatase (ALP) assay (SensoLyte pNPP ALP Assay Kit, AnaSpec, CA, USA). First, the samples were washed twice using a 1× assay buffer. Then, 20 μL of Triton X-100 was added to 10 mL of the 1× assay buffer

and mixed well. This solution was added on top of the samples, and the adherent cells were scraped off. The cell suspension was collected and put into a microcentrifuge tube. The suspension was incubated at 4 °C for 10 min under constant agitation. Then, the suspension was centrifuged at 2500*g* for 10 min at 4 °C. The resultant supernatant was collected for ALP assay and added into a 96-well plate. A 50 μL of the pNPP substrate solution was added to it. The reagents were mixed by gently shaking the plate for 30 s. The reaction was incubated for 45 min at room temperature. In the end, 50 μL of the stop solution was added into each well. The plate was shaken on a plate shaker for 1 min before measuring the absorbance at 405 nm. ALP/cell has been expressed by normalizing with the viable cell number from the MTT assay (OD_{405}/OD_{570}).

2.7. Statistical Analyses.

All data of the in vitro experiments are representative of three biological replicates ($n = 3$). Each of these biological replicates had three technical replicates as well. The data were normally distributed by the Shapiro–Wilk test and were represented as mean ± SD. Statistical analyses were performed in the GraphPad Prism 8 software (CA, USA) using two-way analysis of variance and the Bonferroni posthoc analysis. P values ≤ 0.05 were considered as statistically significant.

3. RESULTS

3.1. Curcumin-Encapsulated Liposomes and 3DP Scaffold Preparation.

Table 1 shows various optimization parameters for developing curcumin-encapsulated liposomes. Solvent media, drug/lipid (D/L) ratios, and hydration media were tailored to optimize the stable bilayer structure with better encapsulation efficiency. The percentage of encapsulation efficiencies was higher in the chloroform–methanol solvent system as compared to the DMSO–*tert*-butanol solvent system. The highest encapsulation efficiency of 68% was achieved with the D/L ratio of 1:15 with water as the hydrating mediim.

The TEM images in Figure 2 showed the most homogeneous structure of liposome with the D/L ratio of 1:15 using DI water as the solvent. The other compositions showed nonhomogeneous, aggregated, and fused liposome particles, which may be attributed to the deformation during preparation, and therefore were excluded from further studies. Figure 3a shows the TEM image of the optimized curcumin-encapsulated liposomes. The sizes of the liposomes incorporated within the scaffold range from 40 to 50 nm, which confirm that they are small unilamellar vesicles. The surface morphology of the 3DP TCP scaffold by FESEM is shown in Figure 3c. After sintering, the designed pore size reduced to 176 ± 4.9 μm, which is clearly visible on the scaffold surface.

3.2. In Vitro Liposome-Encapsulated Curcumin Release.

Figure 4 shows the in vitro curcumin release profile from liposomes for 60 days' time period. The results show that after 60 days, 17% curcumin was released from liposome-encapsulated curcumin, whereas free curcumin showed 30.9% release. Therefore, liposome-encapsulated curcumin exhibited more controlled and sustained release for 60 days compared to only curcumin.

3.3. In Vitro Biological Evaluation.

Seeding efficiency was calculated to evaluate the effect of liposome incorporation on osteoblast cell attachment, as shown in Table 2. Liposome-loaded scaffold showed better seeding efficiency because of the higher surface area compared to the control 3DP TCP scaffold.

Figure 5A shows osteoblast cell viability in uniaxially pressed two-dimensional (2D) TCP disks, 3DP porous TCP scaffold, 3DP porous TCP scaffold with empty liposome, and 3DP porous TCP scaffold with curcumin-encapsulated liposome at days 3, 7, and 11 by MTT assay. The 3DP porous scaffold did not show a significant difference in MTT cell viability compared to the uniaxially pressed 2D TCP disk. However, the results demonstrate a significantly higher number of viable cells in the presence of curcumin-encapsulated liposome compared to control at 3, 7, and 11 days. A clear distinction in cell viability can be seen between control and the curcumin-encapsulated liposome-loaded scaffold in days 7 and 11. The statistical difference is shown to be significant in day 3 ($p = 0.0032$), day 7, and day 11 ($p < 0.0001$). Statistical comparisons between time points show a significant difference, suggesting the effect of curcumin on osteoblast proliferation.

Figure 5B shows osteoblast differentiation at day 11 by ALP assay. ALP expression is evaluated as an osteoblast differentiation marker. The 3DP scaffold showed relatively higher ALP density, compared to the uniaxially pressed 2D TCP disks. The result showed higher osteoblast differentiation in the presence of curcumin-encapsulated liposome-loaded 3DP scaffold compared to control. The statistical difference was significant ($p < 0.0001$) between control and the liposome-loaded scaffold.

Osteoblast cell attachment and growth on control and the liposome-loaded scaffold were analyzed by FESEM, as shown in Figure 5C. Both the control and 3DP TCP samples coated with liposomal curcumin showed healthy osteoblast cell attachment within the substrate at days 3, 7, and 11. Flattened osteoblast cells with complex filopodial prostheses can be seen in liposome-encapsulated curcumin samples at days 7 and 11, which help in cellular extension and better cell attachment to nearby anchor points.

Osteosarcoma (MG-63) cell viability MTT assay was performed on 3DP porous TCP scaffold, 3DP porous TCP scaffold with empty liposome, and 3DP porous TCP scaffold with curcumin-encapsulated liposome at days 3, 7, and 11, as shown in Figure 6A. The result depicts a clear distinction between control (3DP scaffold and 3DP scaffold with only delivery vesicle) and liposome-loaded samples regardless of the time points. The statistical difference of cell viability between the two compositions was significant ($p < 0.0001$) at days 3, 7, and 11. The curcumin-encapsulated liposome-loaded 3DP scaffolds show two- and sevenfold lower cell viability at day 3 and day 7, respectively, compared to control. At day 11, the 368 MG-63 cell viability was almost 96% lower in the presence of curcumin-encapsulated liposome compared to control, as shown in Table 3. The result showed 70% lower cell viability as early as 3 days after cell seeding, which implies that liposomal curcumin-loaded scaffolds have cytotoxic potential against osteosarcoma cell culture.

The proliferation and adhesion of the osteosarcoma cell line were evaluated by morphological characterization by FESEM in Figure 6B. In terms of cell attachment, MG-63 seeded on the control samples shows significantly higher growth, firm attachment, and better spreading. An elongated fibroblast-type morphology with filopodial extension can be seen on the surface of all control samples at days 3 and 7 compared to the scaffolds with curcumin-encapsulated liposomes. At day 11, a layer-like osteosarcoma cell structure can be seen in control, whereas almost none or very poor cell attachment can be seen on the curcumin-encapsulated liposome-loaded 3DP scaffolds.

4. DISCUSSION

Despite the rarity, bone cancer treatment remains a challenge because of its unknown etiology, high metastasis potential, and unsatisfactory survival rate for metastatic and relapse cases.[13] Successful treatment of osteosarcoma requires postsurgical bone defect repair as well as the complete eradication of bone tumor cells in the surrounding tissues.[32,33] In this study, for the first time, a bifunctional bone tissue engineering scaffold has been developed by loading liposome-encapsulated curcumin on bioceramic TCP scaffolds prepared via 3D printing.

Natural biomolecules, like curcumin, are widely researched because of their promising chemopreventive properties without the severe side effects that occur through the utilization of cytotoxic agents.[34] Curcumin has exhibited therapeutic activities against various forms of cancers by inhibiting initiation, progression, invasion, and metastasis of cancer cells. The hydroxyl groups present in the chemical structure of curcumin are essential for its antioxidant activity, whereas the methoxy groups are known to have antiproliferative and anti-inflammatory activities.[35] Liposomal curcumin has been used in the treatment of various forms of cancers in vitro and in vivo, including prostate, breast, liver, lung, cervical, and bone cancers.[36-40] Studies showed that liposomes enhance the biological activity, stability, and anticancer efficacy of curcumin; therefore, curcumin-encapsulated liposome can be considered as an excellent strategy for treating cancers.[25] The mechanism of action of liposomal curcumin involves gradual release of free curcumin from the liposome in the tumor site followed by the uptake of the drug by the malignant cells. In the present study, curcumin-encapsulated liposomes are optimized by tailoring various process parameters such as the D/L ratio, hydrating medium, and the solvent system.

The D/L ratio is a crucial process parameter which determines the capacity of the liposome to encapsulate a drug and thus plays an important role in liposomal optimization.[41] It is affected by the choice of drug and lipids, their composition, as well as the processing method. It regulates the release properties of the drug from the liposome as well as improves the therapeutic efficacy of the encapsulated drug. In this work, we investigated two different D/L ratios, 1:10 and 1:15 curcumin/lipid ratio, of which 1:15 showed a more homogeneous size distribution of the liposome. The result is in accordance with another study, which reported that with increasing D/L ratio, more deformity can be observed in the liposomal morphology. It is recommended to maintain D/L ratio within 0.2, above which membrane disruption and structural deformation can occur.[42] The choice of the lipid bilayer is associated with the stability and permeability of the liposome membrane. In this

work, we have chosen DMPC and DMPG, which are saturated phospholipids and therefore form a rigid, more stable bilayer structure as compared to unsaturated lipids from a natural source, which increases the permeability of the liposome.[29] The lipid bilayer structures are formed when they are hydrated in aqueous solutions. In this study, two different aqueous solutions, PBS and DI water, were used to prepare the liposomes. It has been reported that liposomes exhibit higher zeta potential in DI water compared to phosphate buffer, which implies better colloidal stability in DI water because strong electrostatic repulsion prevents agglomeration of particles. The presence of salt in PBS lowers the zeta potential close to zero and therefore significantly affects liposome stability.[43] The highest encapsulation efficiency is also achieved in the sample having a 1:15 D/L ratio with water as the hydrating medium. The TEM images did not show distinguishable differences comparing the two different solvent systems, thus concluding that they do not have any effect on the liposome structure. The optimized liposomes prepared in this study were unilamellar vesicles with a size of 40–50 nm.

Three-dimensional printing has been extensively used to make synthetic bone graft substitutes because of the precise control over micro- and macro-architecture with interconnected pore geometry, which is crucial for bone ingrowth, nutrient transport, and waste removal. In vivo studies have reported scaffolds made with bioresorbable ceramics like TCP gradually degrade as new bone tissue is formed at the interface and inside the pores.[44] In this work, we fabricated scaffolds using synthesized TCP powders, which required rigorous process optimization. The binder saturation set at 70%, layer thickness of 30 μm, and drying time of 5 s exhibited no layer displacement and crack-free build parts. It is interesting to note that a minimum effective pore size of 100–150 μm is required for bone ingrowth.[45] Keeping this in mind, we have designed a 3DP scaffold with the synthesized TCP ceramics and designed pore size of 200 μm. The sintered pore size was in the range of 176 ± 4.9 μm. Uniformly distributed residual micropores of 10–20 μm can also be seen on the scaffold struts. Our objective is to enhance the functionality of this 3DP scaffold by incorporating curcumin-encapsulated liposome, which will permit the local delivery of the drug in an adequate dose over a desired time period.

The current study evaluated the in vitro chemopreventive properties of liposome-encapsulated curcumin released from a 3DP porous TCP scaffold. The study showed significantly lower MG-63 cell viability in the presence of curcumin-encapsulated liposome. After 3 days of culture, distinctive reduction in cell viability is observed in curcumin-encapsulated liposome-loaded scaffolds by MTT assay. The FESEM images are consistent with the MTT data, showing no sign of cellular attachment in presence of liposome encapsulated curcumin. On the other hand, the entire surface of the control samples is covered with flattened, healthy MG-63 cells. This result is in accordance with the reports which documented all possible mechanistic pathways through which curcumin induces cell death in tumor cells.[2] It has an inhibitory effect on NF-$\kappa\beta$, a transcription factor expressed by tumor cells and thus associated in the pathogenesis of several malignancies, as shown in Figure 7. NF-$\kappa\beta$ is present in the cytoplasm of the cell, and is normally bound to inhibitory kappa beta (I$\kappa\beta$), which keeps it in inactive state. When cells are exposed to free radicals or environmental toxins, I$\kappa\beta$ gets phosphorylated and subsequently degraded. Activated NF-$\kappa\beta$ then travels to the nucleus, where it binds to the DNA and interacts with certain genes,

which may induce osteosarcoma proliferation or osteoblast inhibition. Curcumin blocks this pathway by inhibiting phosphorylation and degradation of I$\kappa\beta$. Inhibition of the NF-$\kappa\beta$ pathway results in apoptosis in the cancer cell line. It also mediates tumor cell death by regulating the cell cycle and inhibiting Wnt/β-catenin signaling, COX2, 5 LOX, growth factors and their receptors, and androgen receptors.[2]

Next, the in vitro bone-forming ability and biocompatibility of this scaffold have been assessed by investigating its effect on osteoblast (hFOB) cell proliferation. Our previous study showed excellent in vitro osteoblast cell formation and in vivo bone regeneration ability of curcumin in a rat distal femur model.[46] To ensure that liposomal encapsulation does not possess any toxic effects to the healthy osteoblast cells, MTT cell viability assay and morphological characterization by FESEM were carried out. The present study showed that curcumin-encapsulated liposome exhibited no toxicity toward the osteoblast or bone-forming cells. The osteoblast cells showed good adhesion, proliferation, and formation of filopodial prostheses on curcumin-encapsulated liposome-coated 3DP TCP scaffolds, as shown by the FESEM images. MTT results also showed higher cell viability of the scaffolds compared to control, suggesting good biocompatibility of the scaffold toward the healthy bone tissue. ALP assay exhibited higher osteoblast-differentiating ability in the presence of liposome--encapsulated curcumin. We have established that liposomal curcumin is available to healthy bone cells in the same extent as the free curcumin, with the added advantage of greater bioavailability. Reviewing all results, the present study establishes an excellent and promising drug delivery device combining curcumin-encapsulated liposome, a natural, nontoxic drug carrier with chemopreventive properties, and 3DP TCP scaffolds with a designed architecture for bone regeneration.

5. SUMMARY

Curcumin has been one of the most highly debated yet extensively researched natural medicines worldwide because of its wide range of therapeutic efficacy. In this work, we have designed a bifunctional scaffold by encapsulating curcumin within a liposome and then incorporating it in a 3DP porous TCP scaffold to establish its application as a potential bone graft substitute after bone tumor resection. The liposomes were optimized by tailoring various parameters such as the D/L ratio, hydrating medium, and the solvent system to synthesize a stable bilayer structure with an encapsulating efficiency of 68%. Furthermore, in vitro curcumin release from the liposome was carried over 60 days, showing 30% release of the drug. More significantly, the presence of liposomal curcumin results in a 96% decrease in in vitro osteosarcoma cell proliferation and viability after 11 days of incubation, compared to control. Results from in vitro osteoblast cell culture demonstrate that liposomal curcumin promotes cell attachment, proliferation, viability, and differentiation. This work establishes the successful fabrication of a novel bifunctional bone tissue engineering scaffold, which not only inhibits bone cancer cells but also promotes formation of healthy bone cells within the porous scaffold, offering a promising drug delivery strategy for the treatment of bone defects after tumor resection.

ACKNOWLEDGMENTS

Researchers would like to acknowledge the financial assistance from NIH [grant # 1R01-AR-066361].

REFERENCES

(1). Nelson KM; Dahlin JL; Bisson J; Graham J; Pauli GF; Walters MA The Essential Medicinal Chemistry of Curcumin. J. Med. Chem 2017, 60, 1620–1637. [PubMed: 28074653]

(2). Ravindran J; Prasad S; Aggarwal BB Curcumin and Cancer Cells: How Many Ways Can Curry Kill Tumor Cells Selectively? AAPS J. 2009, 11, 495–510. [PubMed: 19590964]

(3). Jackson JK; Higo T; Hunter WL; Burt HM The Antioxidants Curcumin and Quercetin Inhibit Inflammatory Processes Associated with Arthritis. Inflammation Res. 2006, 55, 168–175.

(4). Weisberg SP; Leibel R; Tortoriello DV Dietary Curcumin Significantly Improves Obesity-associated Inflammation and Diabetes in Mouse Models of Diabesity. Endocrinology 2008, 149, 3549–3558. [PubMed: 18403477]

(5). Xie L; Li X-K; Takahara S Curcumin Has Bright Prospects for the Treatment of Multiple Sclerosis. Int. Immunopharmacol 2011, 11, 323–330. [PubMed: 20828641]

(6). Anand P; Sundaram C; Jhurani S; Kunnumakkara AB; Aggarwal BB Curcumin and cancer: An ″old-age″ disease with an ″age-old″ solution. Cancer Lett. 2008, 267, 133–164. [PubMed: 18462866]

(7). Kuo M-L; Huang T-S; Lin J-K Curcumin, an Antioxidant and Anti-tumor Promoter, Induces Apoptosis in Human Leukemia Cells. Biochim. Biophys. Acta, Mol. Basis Dis 1996, 1317, 95–100.

(8). Aggarwal BB; Shishodia S; Takada Y; Banerjee S; Newman RA; Bueso-Ramos CE; Price JE Curcumin Suppresses the Paclitaxel-Induced Nuclear Factor- B Pathway in Breast Cancer Cells and Inhibits Lung Metastasis of Human Breast Cancer in Nude Mice. Clin. Cancer Res 2005, 11, 7490–7498. [PubMed: 16243823]

(9). Pillai GR; Srivastava AS; Hassanein TI; Chauhan DP; Carrier E Induction of Apoptosis in Human Lung Cancer Cells by Curcumin. Cancer Lett. 2004, 208, 163–170. [PubMed: 15142674]

(10). Aggarwal BB; Kumar A; Bharti AC Anticancer Potential of Curcumin: Preclinical and Clinical Studies. Anticancer Res. 2003, 23, 363–398. [PubMed: 12680238]

(11). Ficai A; Marques C; Ferreira JM; Andronescu E; Ficai D; Sonmez M Multifunctional materials for bone cancer treatment. Int J Nanomedicine 2014, 9, 2713–2725. [PubMed: 24920907]

(12). González-Fernández Y; Zalacain M; Imbuluzqueta E; Sierrasesumaga L; Patiño-García A; Blanco-Prieto MJ Lipid Nanoparticles Enhance the Efficacy of Chemotherapy in Primary and Metastatic Human Osteosarcoma Cells. J. Drug Delivery Sci. Technol 2015, 30, 435–442.

(13). Luetke A; Meyers PA; Lewis I; Juergens H Osteosarcoma treatment - Where do we stand? A state of the art review. Cancer Treat. Rev 2014, 40, 523–532. [PubMed: 24345772]

(14). Daculsi G; Passuti N; Martin S; Deudon C; Legeros RZ; Raher S Macroporous calcium phosphate ceramic for long bone surgery in humans and dogs. Clinical and histological study. J. Biomed. Mater. Res 1990, 24, 379–396. [PubMed: 2318901]

(15). Vallet-Regí M; Ruiz-Hernández E Bioceramics: From Bone Regeneration to Cancer Nanomedicine. Adv. Mater 2011, 23, 5177–5218. [PubMed: 22009627]

(16). Bose S; Vahabzadeh S; Bandyopadhyay A Bone Tissue Engineering Using 3D Printing. Mater. Today 2013, 16, 496–504.

(17). Bose S; Tarafder S Calcium Phosphate Ceramic Systems in Growth Factor and Drug Delivery for Bone Tissue Engineering: A Review. Acta Biomater. 2012, 8, 1401–1421. [PubMed: 22127225]

(18). Fielding GA; Bandyopadhyay A; Bose S Effects of Silica and Zinc Oxide Doping on Mechanical and Biological Properties of 3d Printed Tricalcium Phosphate Tissue Engineering Scaffolds. Dent. Mater 2012, 28, 113–122. [PubMed: 22047943]

(19). Bigi A; Boanini E Calcium Phosphates as Delivery Systems for Bisphosphonates. J Funct Biomater 2018, 9, 6.

(20). Tarafder S; Bose S Polycaprolactone-Coated 3D Printed Tricalcium Phosphate Scaffolds for Bone Tissue Engineering: In Vitro Alendronate Release Behavior and Local Delivery Effect on In Vivo Osteogenesis. ACS Appl. Mater. Interfaces 2014, 6 (13), 9955–9965. [PubMed: 24826838]

(21). Bose S; Tarafder S; Bandyopadhyay A Effect of Chemistry on Osteogenesis and Angiogenesis Towards Bone Tissue Engineering Using 3D Printed Scaffolds. Ann. Biomed. Eng 2017, 45 (1), 261–272. [PubMed: 27287311]

(22). Banerjee S; Ji C; Mayfield JE; Goel A; Xiao J; Dixon JE; Guo X Ancient Drug Curcumin Impedes 26S Proteasome Activity by Direct Inhibition of Dual-specificity Tyrosine-regulated Kinase 2. Proc. Natl. Acad. Sci U.S.A 2018, 115, 8155–8160. [PubMed: 29987021]

(23). Datta S; Misra SK; Saha ML; Lahiri N; Louie J; Pan D; Stang PJ Orthogonal self-assembly of an organoplatinum(II) metallacycle and cucurbit[8]uril that delivers curcumin to cancer cells. Proc. Natl. Acad. Sci. U.S.A 2018, 115, 8087–8092. [PubMed: 30038010]

(24). Norris I; Sriganth P; Premalatha B Dietary Curcumin with Cisplatin Administration Modulates Tumour Marker Indices in Experimental Fibrosarcoma. Pharmacol. Res 1999, 39, 175–179. [PubMed: 10094841]

(25). Mitra AK; Krishna M In Vivo Modulation of Signaling Factors Involved in Cell Survival. J. Radiat. Res 2004, 45, 491–495. [PubMed: 15635257]

(26). Anand P; Kunnumakkara AB; Newman RA; Aggarwal BB Bioavailability of Curcumin: Problems and Promises. Mol. Pharmaceutics 2007, 4, 807–818.

(27). Bansal SS; Goel M; Aqil F; Vadhanam MV; Gupta RC Advanced Drug Delivery Systems of Curcumin for Cancer Chemo-prevention. Cancer Prev. Res 2011, 4, 1158–1171.

(28). Pochampally R; John V; Alb A; He J; Tan G; Feldman J; Walker R; Frazier T; Penfornis P; Dhule SS Curcumin-loaded γ-cyclodextrin Liposomal Nanoparticles as Delivery Vehicles for Osteosarcoma. Nanomedicine in Cancer; Pan Stanford, 2017; pp 291–322.

(29). Sercombe L; Veerati T; Moheimani F; Wu SY; Sood AK; Hua S Advances and Challenges of Liposome Assisted Drug Delivery. Front. Pharmacol 2015, 6, 286. [PubMed: 26648870]

(30). Feng T; Wei Y; Lee R; Zhao L Liposomal Curcumin and Its Application in Cancer. Int. J. Nanomed 2017, 12, 6027.

(31). Akbarzadeh A; Rezaei-Sadabady R; Davaran S; Joo SW; Zarghami N; Hanifehpour Y; Samiei M; Kouhi M; Nejati-Koshki K Liposome: Classification, Preparation, and Applications. Nanoscale Res. Lett 2013, 8, 102. [PubMed: 23432972]

(32). Wang X; Li T; Ma H; Zhai D; Jiang C; Chang J; Wang J; Wu C A 3D-printed scaffold with MoS2 nanosheets for tumor therapy and tissue regeneration. NPG Asia Mater. 2017, 9, No. e376.

(33). Ma H; Li T; Huan Z; Zhang M; Yang Z; Wang J; Chang J; Wu C 3D Printing of High-strength Bioscaffolds for the Synergistic Treatment of Bone Cancer. NPG Asia Mater. 2018, 10, 1.

(34). Chang R; Sun L; Webster TJ Short communication: Selective Cytotoxicity of Curcumin on Osteosarcoma Cells Compared to Healthy Osteoblasts. Int. J. Nanomed 2014, 9, 461.

(35). Anand P; Thomas SG; Kunnumakkara AB; Sundaram C; Harikumar KB; Sung B; Tharakan ST; Misra K; Priyadarsini IK; Rajasekharan KN; Aggarwal BB Biological Activities of Curcumin and Its Analogues (Congeners) Made by Man and Mother Nature. Biochem. Pharmacol 2008, 76, 1590–1611. [PubMed: 18775680]

(36). Narayanan NK; Nargi D; Randolph C; Narayanan BA Liposome Encapsulation of Curcumin and Resveratrol in Combination Reduces Prostate Cancer Incidence in PTEN Knockout Mice. Int. J. Cancer 2009, 125, 1–8. [PubMed: 19326431]

(37). Hasan M; Belhaj N; Benachour H; Barberi-Heyob M; Kahn CJF; Jabbari E; Linder M; Arab-Tehrany E Liposome Encapsulation of Curcumin: Physico-chemical Characterizations and Effects on MCF7 Cancer Cell Proliferation. Int. J. Pharm 2014, 461, 519–528. [PubMed: 24355620]

(38). Wang L; Zhang J; Cai L; Wen J; Shi H; Li D; Guo F; Wang Y Liposomal curcumin inhibits Lewis lung cancer growth primarily through inhibition of angiogenesis. Oncol. Lett 2012, 4, 107–112.

(39). Sreekanth CN; Bava SV; Sreekumar E; Anto RJ Molecular evidences for the chemosensitizing efficacy of liposomal curcumin in paclitaxel chemotherapy in mouse models of cervical cancer. Oncogene 2011, 30, 3139. [PubMed: 21317920]

(40). Dhule SS; Penfornis P; He J; Harris MR; Terry T; John V; Pochampally R The Combined Effect of Encapsulating Curcumin and C6 Ceramide in Liposomal Nanoparticles Against Osteosarcoma. Mol. Pharmaceutics 2014, 11, 417–427.

(41). Johnston MJW; Edwards K; Karlsson G; Cullis PR Influence of Drug-to-lipid Ratio on Drug Release Properties and Liposome Integrity in Liposomal Doxorubicin Formulations. J. Liposome Res 2008, 18, 145–157. [PubMed: 18569449]

(42). Chountoulesi M; Naziris N; Pippa N; Demetzos C The Significance of Drug-to-lipid Ratio to the Development of Optimized Liposomal Formulation. J. Liposome Res 2018, 28, 249–258. [PubMed: 28627268]

(43). Won DH; Kim SY; Lim GN; Park SN A Study on the Stability of DOPC Liposome. J. Soc. Cosmet. Sci. Korea 2011, 37, 55–60.

(44). Tarafder S; Davies NM; Bandyopadhyay A; Bose S 3D printed tricalcium phosphate bone tissue engineering scaffolds: effect of SrO and MgO doping on in vivo osteogenesis in a rat distal femoral defect model. Biomater. Sci 2013, 1, 1250–1259. [PubMed: 24729867]

(45). Murphy CM; Haugh MG; O'Brien FJ The effect of mean pore size on cell attachment, proliferation and migration in collagen-glycosaminoglycan scaffolds for bone tissue engineering. Biomaterials 2010, 31, 461–466. [PubMed: 19819008]

(46). Bose S; Sarkar N; Banerjee D Effects of PCL, PEG and PLGA polymers on curcumin release from calcium phosphate matrix for in vitro and in vivo bone regeneration. Mater. Today Chem 2018, 8, 110–120. [PubMed: 30480167]

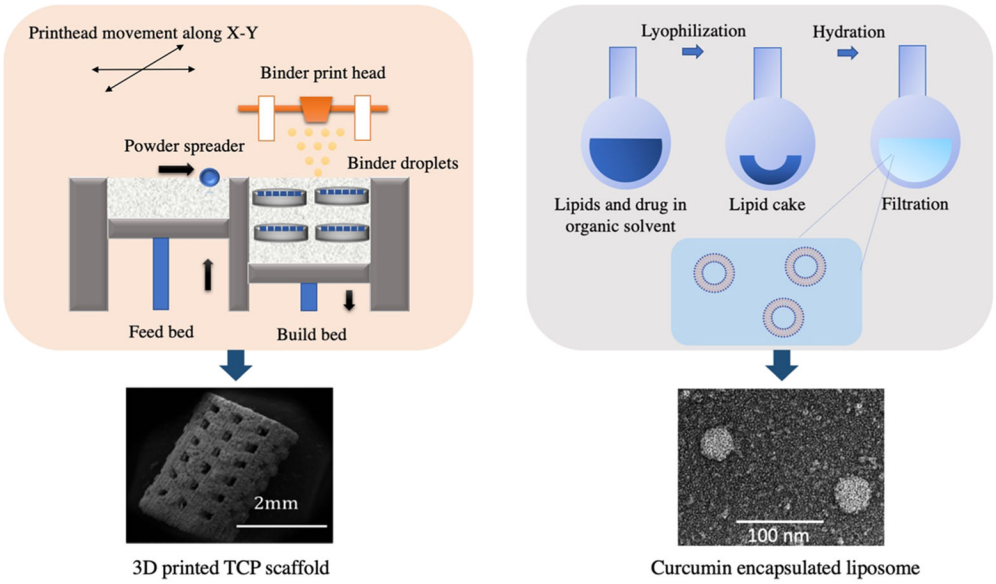

Figure 1.

Schematic illustration of fabricating a bifunctional scaffold. (Left) 3D printing to synthesize a TCP scaffold with a designed porosity; (right) formation of the liposome to enhance the bioavailability of the natural medicinal compound, curcumin, with chemopreventive properties.

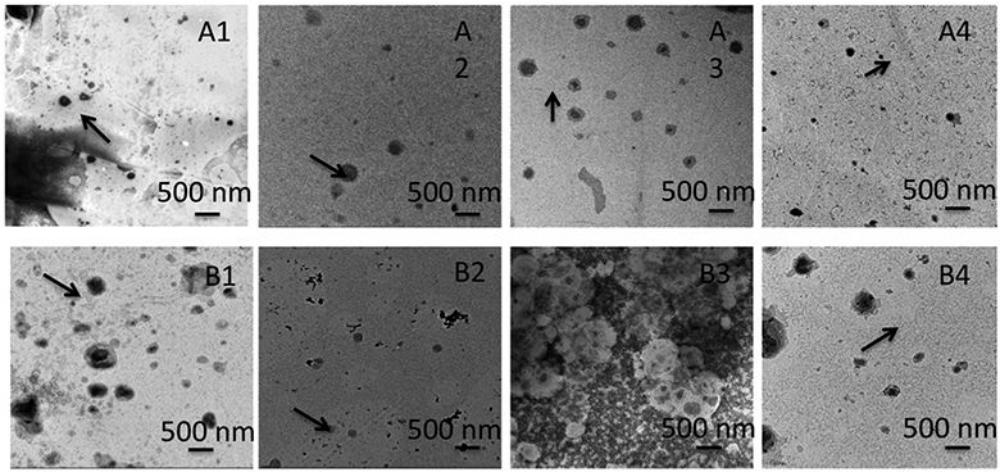

Figure 2.

Different optimization parameters to synthesize curcumin-encapsulated liposomes showing sample A3 with the most homogeneous distribution of curcumin-encapsulated liposome with 68% encapsulation efficiency. Samples A1–A4 indicate liposome formation with the chloroform–methanol solvent system and B1–B4 demonstrate liposomes prepared with the *tert*-butanol–dichloromethane solvent system. A1, A2, B1, and B2 have curcumin/lipid ratio as 1:10, whereas A3, A4, B3, and B4 have curcumin/lipid ratio as 1:15. A1, A3, B1, and B3 liposomes have DI water as the hydrating medium, whereas A2, A4, B2, and B4 liposomes have phosphate buffer as the hydrating medium.

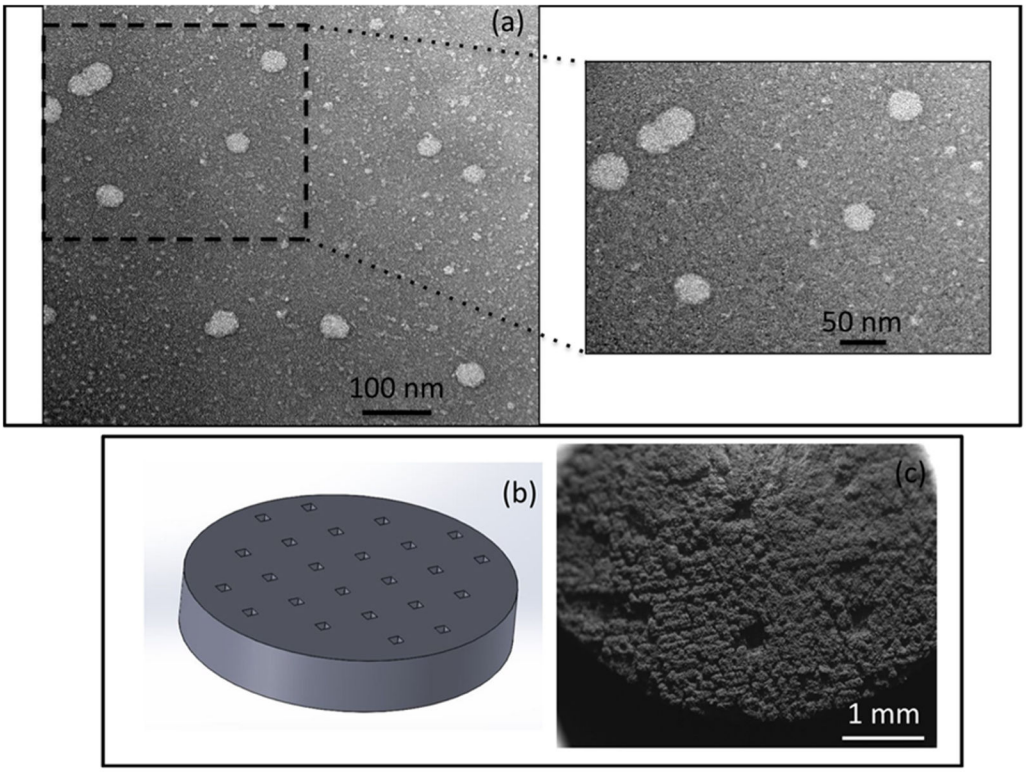

Figure 3.

Curcumin-encapsulated liposomes and 3DP scaffold preparation. (a) TEM images of curcumin-encapsulated liposomes show a homogeneous distribution of liposomes with sizes in the range 40–50 nm. (b) CAD file of the 3DP disk with a designed pore size of 200 μm. (c) SEM images of the 3DP scaffold showing sintered pore size of 176 ± 4.9 μm.

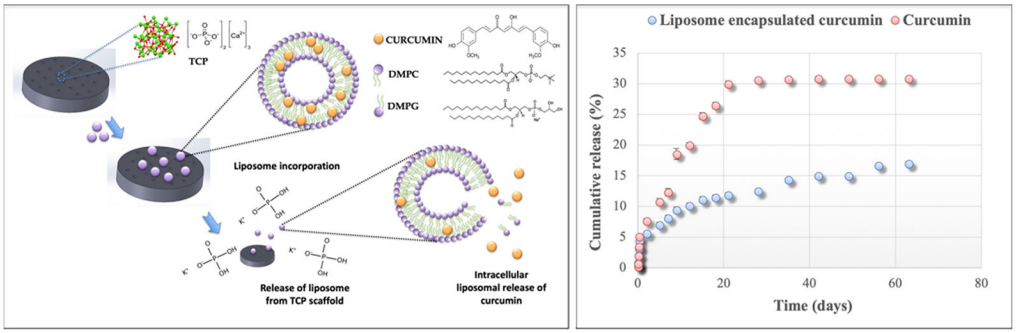

Figure 4.

(Left) Chemical structure of the 3DP scaffold and liposome-encapsulated curcumin is demonstrated. The liposome contains DMPC and DMPG, which form the phospholipid bilayer, and curcumin is trapped within the hydrophobic region of the liposome. In the presence of a buffer medium or an extracellular medium, liposome release takes place, followed by the intracellular release of curcumin from the liposome. (Right) In vitro liposome-encapsulated curcumin release: controlled release of curcumin is shown from liposomes, exhibiting 17% release after 60 days, whereas free curcumin showed a 30.9% release.

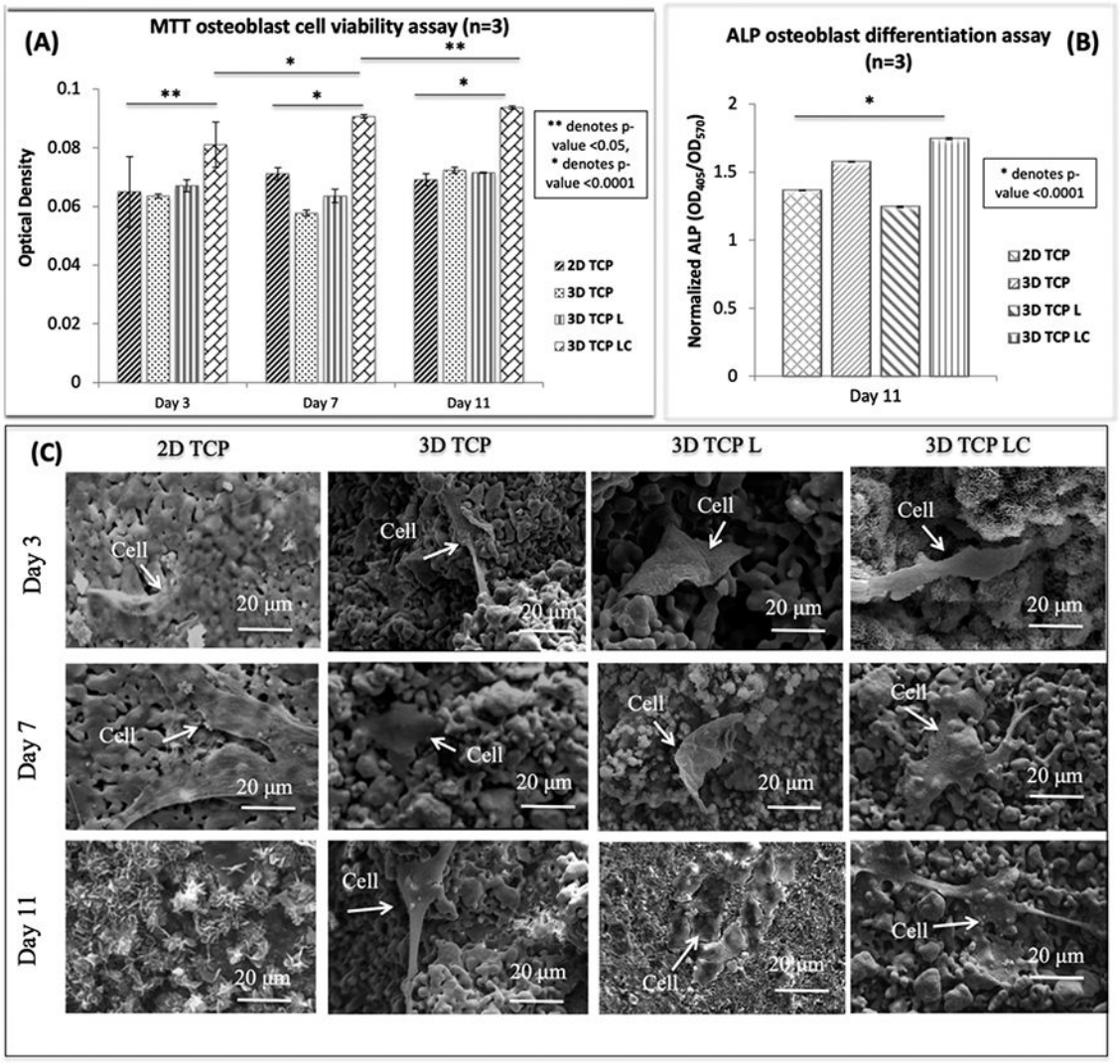

Figure 5.

Effects of curcumin-encapsulated liposome-coated 3DP scaffolds on osteoblast cells [2D TCP: uniaxially pressed 2D TCP disks; 3D TCP: 3DP porous TCP scaffold; 3D TCP L: 3DP porous TCP scaffold with empty liposome; 3D TCP LC: 3DP porous TCP scaffold with curcumin-encapsulated liposome]: (A) MTT osteoblast cell viability assay ($n = 3$) after 3, 7, and 11 days of culture showing curcumin encapsulated liposome-coated samples with higher cell viability compared to the control samples. Statistical analysis shows a significant difference between control and test samples [** denotes p value < 0.05, * denotes p value < 0.0001]. (B) ALP osteoblast cell differentiation assay ($n = 3$) after day 11 of culture showing curcumin-encapsulated liposome-coated samples showed much higher osteoblast cell differentiation compared to the control samples (untreated 3DP scaffolds) [* denotes p value < 0.0001, a significant difference between control and the test sample]. (c) Curcumin-encapsulated liposome exhibited no toxicity toward the osteoblast or bone-forming cells. FESEM images of osteoblast cell culture with curcumin-encapsulated liposome-coated 3DP

scaffold showing good adhesion, proliferation, and formation of filopodia on the sample surface.

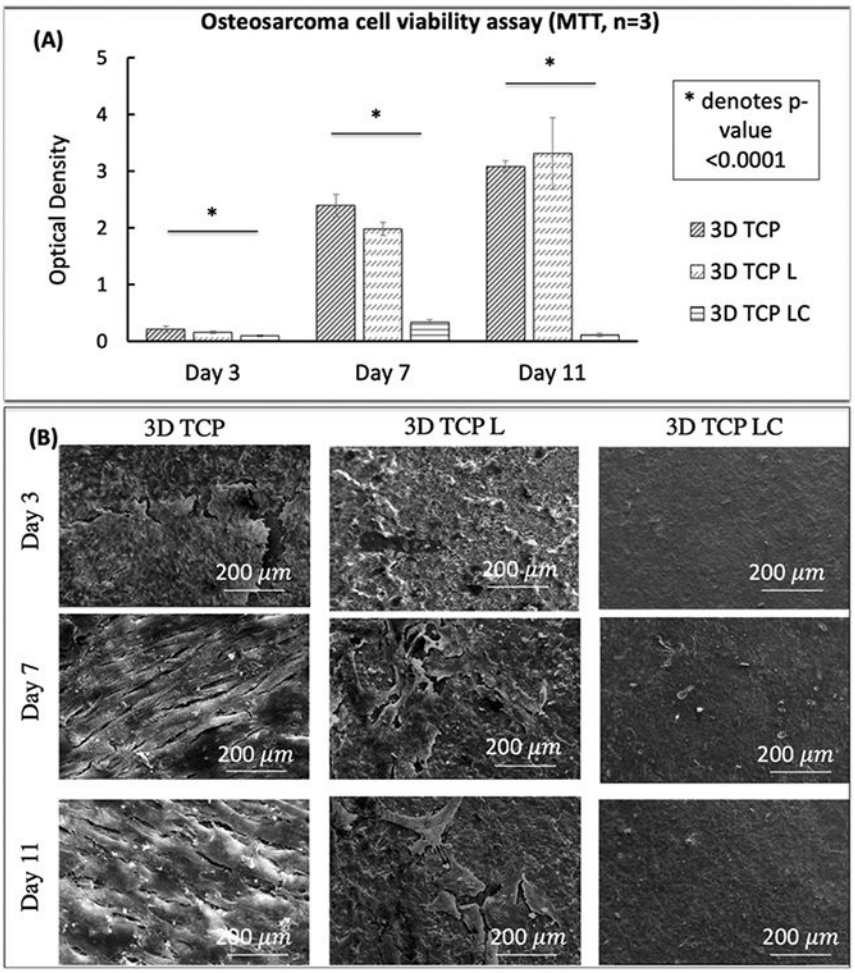

Figure 6.

Effects of curcumin-encapsulated liposome-coated 3DP scaffolds on osteosarcoma cell line [3D TCP: 3DP porous TCP scaffold; 3D TCP L: 3DP porous TCP scaffold with empty liposome; 3D TCP LC: 3DP porous TCP scaffold with curcumin-encapsulated liposome]: (A) MTT osteosarcoma cell viability assay ($n = 3$) after 3, 7, and 11 days of culture showing curcumin-encapsulated liposome-coated samples with much higher cell viability compared to the control scaffolds (untreated 3DP scaffolds and 3DP scaffolds with empty liposome) [* denotes p value < 0.0001]. (B) SEM images of osteosarcoma cell culture with curcumin-encapsulated liposome-coated 3DP scaffold showing an absence of osteosarcoma cells compared to the control samples (untreated 3DP scaffolds and 3DP scaffolds with empty liposome).

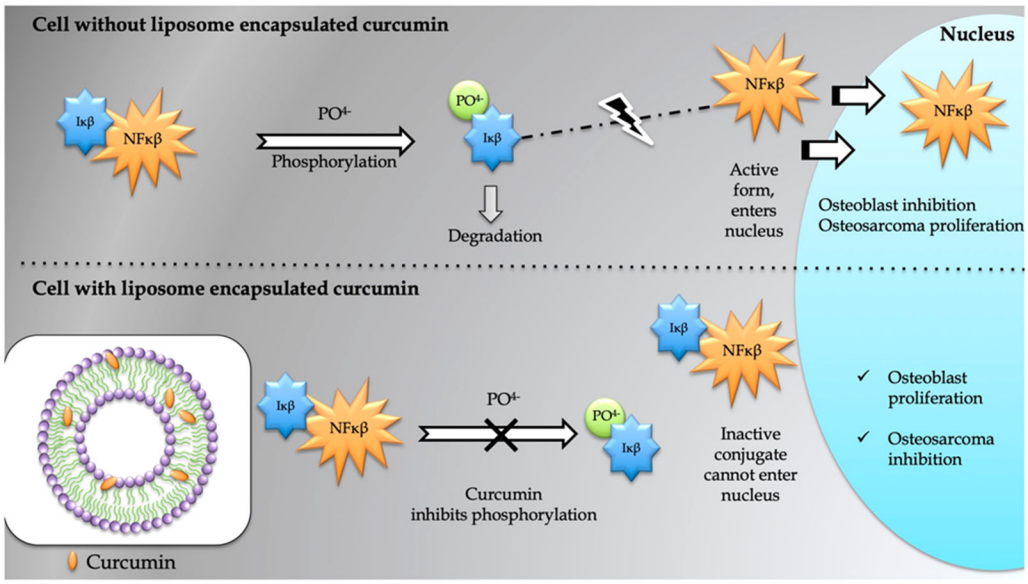

Figure 7.

Curcumin inhibits phosphorylation and degradation of the nuclear factor-κβ inhibitor (Iκβ), which leads to the formation of an inactive conjugate NF-κβ–Iκβ. The mechanism of action shows that the suppression of NF-κβ pathway may positively influence osteoblast differentiation and prevent osteosarcoma proliferation.

Table 1.

Different Optimization Parameters To Synthesize Curcumin-Encapsulated Liposomes Showing Sample A3 with the Most Homogeneous Distribution of Curcumin-Encapsulated Liposome with 68% Encapsulation Efficiency

samples	solvent system	curcumin/lipid ratio	hydrating media	encapsulation efficiency (%)
A1	chloroform–methanol	1:10	DI water	65.3
A2			phosphate buffer	52.7
A3		1:15	DI water	68
A4			phosphate buffer	61.2
B1	*tert*-butanol–dichloromethane	1:10	DI water	51
B2			phosphate buffer	44
B3		1:15	DI water	45.2
B4			phosphate buffer	48.1

ACS Appl Mater Interfaces. Author manuscript; available in PMC 2022 January 27.

Table 2.

Seeding Efficiency of the 3DP Porous Scaffold and 3DP Scaffold with Liposome after 12 h of Seeding Using MTT Assay ($n = 3$)

samples	seeding efficiency (%)
3DP scaffold	53.31 ± 1.96
3DP scaffold with liposome	61.19 ± 1.43

Table 3.

Percentage Cell Viability of 3DP Scaffold with Liposome after 3, 7, and 11 Days of Seeding Using MTT Assay [% Viability < 70% Implies the Agent has Cytotoxic Potential]

MG-63 cell culture time point	% viable cells (cytotoxicity)
day 3	45.41%
day 7	14.18%
day 11	3.56%